Beiträge zur Algebra und Geometrie
Contributions to Algebra and Geometry
Volume 46 (2005), No. 1, 19-42.

Symmetry Groups and Fundamental Tilings for the Compact Surface of Genus 3^-

2. The normalizer diagram with classification

Emil Molnár **Eleonóra Stettner**

Inst. Math., Dept. Geometry, Budapest Univ. Techn. Econ.
H-1521 Budapest XI. Egry J. u. 1
e-mail: emolnar@mail.bme.hu

Inst. Math. and Inf. Tech., Dept. Applied Math. and Physics, University of Kaposvár
H-7200 Kaposvár Guba S. u. 40
e-mail: stettner@mail.atk.u-kaposvar.hu

Abstract. This is a continuation of [16] where the complete diagram of metric normalizers of the fundamental group $\mathbf{G}=\otimes^3$ in Isom H^2 will be determined (Table 2). Thus we completely classify the symmetry groups $\mathbf{N}/\mathbf{G}$ of the 3^- surface, i.e. the connected sum of 3 projective planes, into 12 normalizer classes, up to topological equivariance, by the algorithm for fundamental domains, developed in [9], [10], [11] and [15], aided by computer. Our algorithm is applicable for any compact surface with exponential complexity by the genus g.

1. Introduction

The possible isometry groups of compact non-orientable surfaces have seemingly not been investigated intensively yet. The orientable Riemann surfaces, however, have a vast literature (see e.g. [1], [4], [8], [15], [18], [19]). A Riemann surface of genus g^+ ($g \geq 2$) may have an orientation preserving isometry group $\mathbf{N}/\mathbf{G}$ of finite order at most $84(g-1)$, as it is well-known [19]. Here $\mathbf{G}=\mathrm{O}^g$ is the fundamental group of the connected sum of g tori and $\mathbf{N}$ is a normalizer group of $\mathbf{G}$ in Isom^+H^2, i.e. in the orientation preserving isometry group of the hyperbolic plane. This estimate is sharp for some g's, e.g. for $g = 3$ first (see e.g. [8]).

By our knowledge, an analogous estimate is not proved for a non-orientable compact surface of genus $g = 3$ whose universal covering space, as above, may have a hyperbolic metric of constant negative curvature, fixed to $K = -1$ in the following.

We may speak about a g^- surface $H^2/\mathbf{G}$, for simplicity, where a discontinuous fixed-point-free isometry group, denoted and presented by

$$\mathbf{G} = \otimes^g := (a_1, a_2, \dots, a_g - a_1a_1a_2a_2\dots a_ga_g\ (=1))\ g \geq 3, \tag{1.1}$$

acts on the hyperbolic plane H^2. We shall use the Conway-Macbeath denotation of orbifold signature as for any corresponding hyperbolic normalizer $\mathbf{N}$ and for the orbit space (orbifold surface) $H^2/\mathbf{N}$ as well. It is well-known [19] that the signature determines the group up to homeomorphism equivariance (see Section 3). Moreover, isomorphic groups, acting discontinuously on E^2 or on H^2, will necessarily be equivariant. That means, e.g.

$$\mathrm{O}^g\ h_1, \dots, h_r * h_{11}, \dots, h_{1c_1} * \dots * h_{q1}, \dots, h_{qc_q} \tag{1.2}$$

denotes an orientable orbifold surface as connected sum of g tori; with r rotation centres of orders $h_1, \dots, h_r$ (≥ 2), respectively, up to a permutation; with q boundary components with c_i dihedral corners of orders $h_{i1}, \dots, h_{ic_i}$ (≥ 2), respectively, up to a cyclic permutation on the i-th ($1 \leq i \leq q$) component, according to the fixed positive orientation. The boundary components, separated by stars ($*$), may be permuted, too. For non-orientable orbifolds

$$h_1, \dots, h_r * h_{11}, \dots, h_{1c_1} * \dots * h_{q1}, \dots, h_{qc_q} \otimes^g \tag{1.3}$$

means a connected sum of g cross caps, i.e. projective planes, the other data are as above, but the cyclic order of the dihedral corners may be reversed on any boundary component independently.

Of course, any date above can be missing. The empty signature means the sphere with the trivial group action. In our Tables 1–4 of normalizers e.g. **N=24$*$** denotes the orbifold surface of genus zero (a topological sphere), with two rotation centres of order 2 and 4; with one boundary component without any dihedral corner on it. This can be described by a fundamental domain F_N in Fig. 2.b, and by a corresponding presentation.

$$\mathbf{N} = \mathbf{24}* = (h_1, h_2, m - h_1^2, h_2^4, m^2, mh_1h_2mh_2^{-1}h_1) \tag{1.4}$$

as a general algorithmical scheme (Poincaré algorithm [12]) shows. Another normalizer **N=2$*\otimes$** describes the orbifold with one cross cup, with one rotation centre of order 2, with one boundary component without any dihedral corner on it. Fig. 3 shows a fundamental domain $\mathrm{F}_{\mathbf{N}}$ and the presentation

$$\mathbf{N} = \mathbf{2}*\otimes = (m, h, t, g - m^2, h^2, mtmt^{-1}, hggt) \tag{1.5}$$

(see [16] case 2. **aabcbC**).

In Table 2 you see our result that the surface 3^- has 2 maximal, i.e. not extendable, symmetry groups: $*$**2223/G** of order 12 and $*$**2224/G** of order 8. The other groups **N/G** (**G**= $\otimes^3$)

are their subgroups, having a lattice structure. This is in (a rough) analogy to the 17 classes of the Euclidean (E^2) plane crystallographic groups $\mathbf{N}/\mathbf{T}$, where

$$\mathbf{N_1} = \mathbf{p6mm} = *\mathbf{236} \quad \text{and} \quad \mathbf{N_2} = \mathbf{p4mm} = *\mathbf{244} \tag{1.6}$$

are the maximal normalizers (without additional translation) of the torus group

$$\mathbf{T} = \mathbf{p_1} = \mathrm{O} = (\mathrm{a}_1, \mathrm{b}_1 - \mathrm{a}_1\mathrm{b}_1\mathrm{a}_1^{-1}\mathrm{b}_1^{-1}\ (=1)). \tag{1.7}$$

Therefore, our classification can be considered as an extension of the 17 discontinuous E^2 groups to those of the other compact surfaces of hyperbolic metric. The computer implementation of [15] has listed the 65 combinatorial fundamental domains (Table 1) for the 3^- surface $H^2/\otimes^3$. The general algorithm, for finding all the fundamental domains for g^- surface in [9, 10], [11] is based on the fixed-point-free pairings on a $2g$-gon, with one vertex class, at least one side pairing is orientation reversing, then comes a tree graph construction with additional vertices. Along this graph the surface is cut and unfolded onto a topological polygon at most of $6(g-1)$ sides, at most of $2(g-1)$ vertex classes, in each class 3 vertices at least (this process is indicated in Fig. 4.a–b).

In [16] the 8 hexagonal domains with its neighbourhoods provided us the 6 cases of 3 generator systems of locally minimal closed geodesics (Fig. 3). Now, the possible isometries of H^2, transforming these systems onto themselves, extend $\mathbf{G}=\otimes^3$ to all possible normalizers $\mathbf{N}$ with a corresponding fundamental domain $\mathrm{F}_\mathbf{N}$ whose finitely many representative $\mathbf{N}/\mathbf{G}$-images necessarily tile at least one from the 65 domains. Our task is the procedure to find $\mathrm{F}_\mathbf{N}$ and $\mathbf{N}$ from $\mathrm{F}_\mathbf{G}$.

In such a way we obtain not only the possible groups $\mathbf{N}/\mathbf{G}$ but also the possible normalizer tilings of the 3^- surface $H^2/\mathbf{G}$ up to a combinatorial (topological) equivalence of domains $\mathrm{F}_\mathbf{N}$. Of course, different fundamental domains for $\mathbf{G}=\otimes^3$ may induce the same domain for a normalizer $\mathbf{N}$, i.e. equivariant tilings for the 3^- surface $H^2/\mathbf{G}$ (see e.g. Fig. 1. c–e, 4. a–b). But combinatorially different $\mathrm{F}_\mathbf{N}$'s for fixed $\mathbf{N}$ will be distinguished as providing different tilings for $H^2/\mathbf{G}$. Our Table 1 lists the typical maximal normalizer(s) $\mathbf{N}$ for each $\mathrm{F}_\mathbf{G}$, sometimes not uniquely, that can be tiled by an appropriate $\mathrm{F}_\mathbf{N}$. By Table 2 we can turn to other fundamental tilings by symmetry breakings of subgroup actions.

Then the complete classification of fundamental tilings with $\mathrm{F}_\mathbf{N}$'s for the 3^- surface by [9] is relatively easy but it would be too lengthy to list here. The authors will send it on request of the interested reader. As an information we list all the combinatorially different polygon symbols $\mathrm{F}_\mathbf{N}$ in Table 3 for occurring normalizers $\mathbf{N}$ by [11].

We formulate the main results in our

Theorem. *The* 3^- *surface, as a connected sum of* 3 *projective planes, allows hyperbolic* (H^2) *metric structures such that* 12 *isometry groups* $\mathbf{N}/\mathbf{G}$ *can act on the* 3^- *surface, induced by normalizers* $\mathbf{N}$ *of the fundamental group* $\mathbf{G} = \otimes^3$ *in the isometry group of* H^2, *up to homeomorphism equivariance. These* 12 *normalizers* $\mathbf{N}$ *provide* $65 + 58$ *fundamental tilings for our* 3^- *surface* $H^2/\mathbf{G}$ (Tables 1–4).

2. The general strategy by illustrating examples

As it has already been mentioned in [16], the general construction of universal covering allows us to consider any compact non-orientable surface as an orbit structure $\Pi^2/\mathbf{G}$. Here Π^2 is a complete simply connected plane, one of S^2, E^2, H^2, i.e. the sphere, Euclidean and hyperbolic plane, respectively, and $\mathbf{G}$ is an isometry group acting on Π^2 freely and with a compact fundamental domain $\mathrm{F}_{\mathbf{G}}$ (a topological polygon), endowed with consecutive side pairings (Fig. 1. a–b)

$$a_i : s_{a_i}^{-1} \to s_{a_i}, \quad a_i^{-1} : s_{a_i} \to s_{a_i}^{-1}, \quad 1 \le i \le g \tag{2.1}$$

of orientation reversing isometries (glide reflections). This leads to the canonical presentation of the fundamental group $\mathbf{G}$ as described in (1.1).

S^2, $g = 1$ leads to the projective plane,
E^2, $g = 2$ leads to the Klein bottle,
H^2, $g \ge 3$ leads to the other non-orientable compact surfaces, e.g. to our 3^- surface, being discussed. (2.2)

A glide reflection as a product of 3 line reflections

$$a = m_1 m_2 m = m_1 m m_2 = m m_1 m_2, \quad m \perp m_1, m_2 \tag{2.3}$$

has an invariant line denoted by m (for simplicity) serving locally (in a small tape) minimal closed geodesics for the surface $\Pi^2/\mathbf{G}$, represented by $\mathrm{F}_{\mathbf{G}}$ as well. Any orbit

$$P^{\mathbf{G}} := \{P^\gamma \in \Pi^2 : \ \gamma \in \mathbf{G} \text{ by } (1.1)\} \tag{2.3}$$

is a point of $\Pi^2/\mathbf{G} \sim F_{\mathbf{G}}$, and the metric, the topology of the surface can be derived naturally. Note that the sides of $\mathrm{F}_{\mathbf{G}}$ may be continuous curves, not only straight lines.

Of course, $\Pi^2/\mathbf{G}$ may have many fundamental domains according to other presentation of $\mathbf{G}$ which may lead to other metrics of the surface $\Pi^2/\mathbf{G} \sim F_{\mathbf{G}}$ with other symmetry groups. These cause the difficulties of the problem.

Fig. 1. a shows us the seemingly most symmetric tiling of H^2 by (1.1), $g = 3$, derived from the canonical regular hexagons 6/1. The barycentric subdivision into $(\pi/2, \pi/6, \pi/6)$ triangles with $\cdots$ dotted, - - - dashed, and — continuous side lines indicates also the σ_0-, σ_1-, σ_2-adjacencies, respectively, for a D-symbol, described also in [16] (see [7] as well).

The polygon symbol **aabbcc** induces also the side pairing generators by (2.1). After having distinguished an identity (denoted by 1) fundamental domain $\mathrm{F}_{\mathbf{G}} = F$, its neighbouring images will be $\mathrm{F}^{a_1^{-1}}, F^{a_1}, \dots, F^{a_3^{-1}}, F^{a_3}$ and so on: $\mathrm{F}^{a_i\gamma}$ denotes the γ-image of F^{a_i}, i.e. the a_i-neighbour of F^γ along the side a_i^γ, i.e. $(F^\gamma)^{\gamma^{-1}a_i\gamma}$ the image of F^γ under the γ-conjugate of a_i. These hold also for barycentric triangles and their orbits. The formula

$$(\sigma_i C)^\gamma = \sigma_i(C^\gamma) \tag{2.4}$$

indicates an associativity law for any barycentric triangle C, $i = 0, 1, 2$; $\gamma \in \mathbf{G}$ (e.g. $\sigma_0(3^{a_1^{-1}}) = (\sigma_0 3)^{a_1^{-1}} = 4^{a_1^{-1}}$ in Fig. 1.b).

In Fig. 1.a and its fragment in Fig. 1.b there are drawn the invariant lines of a_i's and of their conjugates by dick — lines. These represent the locally minimal closed geodesics of the surface $H^2/\mathbf{G} \sim F_{\mathbf{G}}$. E.g. M_1M_2 is such a line of the midpoint polygon $M_1 \dots M_{2g}$ of the fundamental polygon $V_1 \dots V_{2g}$.

It is easy to see now that the diagonals of $V_1 \dots V_{2g}$ and the side lines of $M_1 \dots M_{2g}$ will be the reflection lines for the generating line reflections of the maximal normalizer for $\mathbf{G} = \otimes^3$. The reflection lines dissect the barycentric triangles, e.g. we denote them in Fig. 1.b by

$$m_{12} : 2 \leftrightarrow 2', \quad m_{2g1} : 1 \leftrightarrow 1' \tag{2.5}$$

as reflections, moreover, m_1 in OV_1 and m_{2g} in OV_{2g} determine the fundamental domain $\mathrm{F}_{\mathbf{N}} = (1, 2)$ of this maximal normalizer $\mathbf{N}{=}{*}\mathbf{2223}$, $|\mathbf{N}/\mathbf{G}| = 12$.

Remark 2.1. In Fig. 1.b we have indicated the general construction scheme for any g^- surface, $g \geq 3$. This shows our natural general conjecture that

$\mathbf{N}_{g^-} = *\mathbf{222g}$ with $|\mathbf{N}/\mathbf{G}| = 4g$,
as reflection group in the $(\pi/2, \pi/2, \pi/2, \pi/g)$ quadrangle,
is the maximal normalizer of $\mathbf{G} = \otimes^g$
in the isometry group Isom H^2 of the hyperbolic plane. (2.6)

We intend to prove this conjecture in a forthcoming paper.

Fig. 1.c–e show the typical phenomena of our topic. Fig. 1.a with the tiling of $\mathrm{F}_{\mathbf{N}}$- images under $\mathbf{N} = *\mathbf{2223}$ provides also other fundamental domains for $\mathbf{G} = \otimes^3$, tiled by $\mathrm{F}_{\mathbf{N}}$- images. See also Fig. 4.a–b for 12-gonal domains.

Expressing the side pairing generators of $\mathrm{F}_{\mathbf{G}}$ from those of $\mathrm{F}_{\mathbf{N}}$, by $\mathbf{G}\varpi\mathbf{N}$, we obtain the homomorphism

$$\mathbf{N} \to \mathbf{N}/\mathbf{G}, \quad n \to n\mathbf{G} = \mathbf{G}n =: \overline{n} \tag{2.7}$$

as a *criterion of correctness of* $\mathrm{F}_{\mathbf{N}}$. E.g. $a_1 = m_{61}m_{12}m_1$, $m_{12} \perp m_{61}$, m_1 (Fig. 1.b, $g = 3$), induces $\overline{m}_{61} = \overline{m}_1\overline{m}_{12} = \overline{m}_{12}\overline{m}_1$, denoted also by $m_{61} \sim m_{12}m_1 = M_{12}$. Here $M_{12} = m_{12}m_1 = m_1m_{12}$ is the point reflection in the point $M_{12} := m_1 \cap m_{12}$. The geometric presentation of $\mathbf{N}$ by $\mathrm{F}_{\mathbf{N}}$

$$\mathbf{N}{:=}{*}\mathbf{2223}{=}(m_1, m_{12}, m_{61}, m_6 — m_1^2, m_{12}^2, m_{61}^2, m_6^2, (m_1m_{12})^2, (m_{12}m_{61})^2, (m_{61}m_6)^2, (m_6m_1)^3), \tag{2.8}$$

as a Coxeter's reflection group, and the homomorphism above provide us the geometric presentation.

$$*\mathbf{2223}/\mathbf{G} := \mathbf{D}_3 \times \mathbf{D}_1 = (\overline{m}_6, \overline{m}_1, \overline{M}_{12} — \overline{m}_6^2, \overline{m}_1^2, \overline{M}_{12}^2, (\overline{m}_6\overline{m}_1)^3, (\overline{m}_1\overline{M}_{12})^2, (\overline{m}_6\overline{M}_{12})^2) \tag{2.9}$$

as a direct product of two dihedral groups. Only the last relation needs checking, but we have just started with this.

Fig. 2.a shows the other most symmetric $\mathbf{G}$-tiling by the fundamental octagon 8/22 with symbol **abcdaBcD** with two vertex $\mathbf{G}$-classes, 4 vertices in each. This $\mathrm{F}_{\mathbf{G}}$ provides the side pairing generators

$$\begin{aligned} &g_1 : s_{a^{-1}} \to s_a, && g_3 : s_{c^{-1}} \to s_c \text{ as glide reflections} \\ &t_2 : s_b \to s_B, && t_4 : s_d \to s_D \text{ as translations} \end{aligned} \tag{2.9}$$

with the corresponding invariant line segments, as locally minimal closed geodesics, g_1, g_2 are orientation reversing, t_2 and t_4 preserve the orientation.

A translation is a product of two line reflections or of two point reflections as

$$\begin{aligned} t = m_1 m_2 = m_1 m m m_2 = A_1 A_2 \text{ with } m \perp m_1, m_2, \\ m_1 m = m m_1 = A_1, \ m m_2 = m_2 m = A_2 \end{aligned} \tag{2.10}$$

show, in general. The line $m = A_1 A_2$ contains the locally minimal closed geodesics.

$F_{\mathbf{G}}$ provides the presentation (the relations for the vertex classes $\circ$ and $\bullet$, respectively):

$$\mathbf{G} = (g_1, t_2, g_3, t_4 \ - \ \circ : g_1 t_2^{-1} g_3 t_2^{-1} (= 1), \ \bullet : g_1 t_4 g_3^{-1} t_4). \tag{2.11}$$

$F_{\mathbf{G}}$ can be chosen as a regular octagon with $\pi/2$ angles. Then the reflections in the sides of $F_{\mathbf{N}} = (1, 16)$ generate

$$\begin{aligned} &\mathbf{N} = *\mathbf{2224} := \\ &(m_1, m_2, m_3, m_4 \ - \ m_1^2, m_2^2, m_3^2, m_4^2, (m_1 m_2)^2, (m_2 m_3)^2, (m_3 m_4)^2, (m_4 m_1)^4), \\ &|\mathbf{N}/\mathbf{G}| = 8, \end{aligned} \tag{2.12}$$

the maximal normalizer, mapping the invariant line system of the generators onto itself. The expressions

$$g_1 = m_2 m_1 m_4 m_1 m_4, \quad t_4^{-1} = m_3 m_1 m_4 m_1 \tag{2.13}$$

induce the homomorphism $\mathbf{N} \to \mathbf{N}/\mathbf{G}$, $m_2 \sim (m_1 m_4)^2 = (m_4 m_1)^2$, $m_3 \sim m_1 m_4 m_1$ and

$$*\mathbf{2224}/\mathbf{G} := \mathbf{D}_4 = (\overline{m}_1, \overline{m}_4 \ - \ \overline{m}_1^2, \overline{m}_4^2, (\overline{m}_1 \overline{m}_4)^4) \tag{2.14}$$

of order 8. Fig. 2.a shows the barycentric subdivision of $F_{\mathbf{G}}$-tiling and a neighbourhood of the two typical non-**G**-image vertices. Thus we obtain the 6/5 hexagon of polygon symbol **a'b'a'c'b'c'** whose angles are $\pi/2, \pi/4, \pi/4, \pi/2, \pi/4, \pi/4$ at the vertices **G**-equivalent to the octagon centre O. We see that the 6/5 hexagon (Fig. 3) with $\pi/3$ angles and its **G**-tiling with normalizer **N**= **2∗222** can be extended by a combinatorial (equivariant, **G**-preserving homeomorphic change) to a more symmetric **G**-tiling with richer normalizer ∗**2224**, but the domains then do not tile the regular hexagon.

Remark 2.2. Our construction scheme can be generalized again for regular $4(g-1)$-gon with side pairing glide reflection and translation each of number $g-1$, with $g-1$ vertex classes, 4 vertices in each with $\pi/2$ angles. Then $\mathbf{N}_{g^-} = *\mathbf{222}[\mathbf{2}(\mathbf{g}-\mathbf{1})]$ is conjectured as second richest normalizer.

In Fig. 2.b there are indicated the 3 possibilities of index 2 subgroups **24∗, ∗22222, 2∗222**, each normalizing $\otimes^3$, whose fundamental domains contain two ones of ∗**2224**.

Fig. 5 shows how to derive the maximal subgroups, of index 2 and 3, respectively (invariant: —— or not: - - - in Table 2), of normalizer ∗**2223** as well. Further maximal subgroups of **23∗** in Fig. 6 and of **2∗33** in Fig. 7 are indicated by our conventions, followed here for illustration.

3. The completeness proof of our classification

The basic tool is the algorithmic enumeration of fundamental domains for any compact plane group of given signature [9], [10], [11], namely, for the fundamental group $\mathbf{G}$ of a compact surface and for its normalizer $\mathbf{N}$ (see Tables 1–3). The diagram

$$\begin{tikzcd}
\Pi_j^2 \ni P_j \arrow[r, "g_i \in \mathbf{G} < \operatorname{Isom}\Pi_j^2"] \arrow[dd, "N_k \ni n_k"'] & P_j^{g_i} \in \Pi_j^2 (= H^2) \arrow[d, "n_k \in N_k < \operatorname{Isom}\Pi_j^2"] \\
 & P^{g_i n_k} \arrow[d, equal] \\
\Pi_j^2 \ni P_j^{n_k} \arrow[r, "g_i' \in \mathbf{G}_i"'] & P_j^{n_k g_i'} \in \Pi_j^2
\end{tikzcd} \tag{3.1}$$

symbolizes how the fundamental group $\mathbf{G}_i = \{g_i\}$ acts on the universal covering plane $\Pi_j^2 = \{P_j\}$ to form the orbit plane $\Pi_j^2/\mathbf{G}_i$ as a surface, and how a $\mathbf{G}_i$-normalizer $\mathbf{N}_k < \operatorname{Isom}\Pi_j^2$, mapping any $\mathbf{G}_i$-orbit $P_j^{\mathbf{G}_i}$ onto another one $P_j^{n_k\mathbf{G}_i} = P_j^{\mathbf{G}_i n_k}$ for any $n_k \in \mathbf{N}_k$, induces an isometry group $\mathbf{G}_i/\mathbf{N}_k$ of the surface:

$$\mathbf{G}_i \lhd \mathbf{N}_k < \operatorname{Isom}\Pi_j, \text{ thus } n_k\mathbf{G}_i = \mathbf{G}_i n_k \in \mathbf{G}_i/\mathbf{N}_k \tag{3.2}$$

as usual. Here Π_j^2 is either S^2 or E^2 or H^2. $\mathbf{G}_i$ and $\mathbf{N}_k$ will be determined up to a homeomorphism equivariance by the signature described in the introduction.

Definition. *The action of $\mathbf{G}_1$ on Π_1^2 is φ-equivariant to that of $\mathbf{G}_2$ on Π_2^2 if there is a homeomorphism*

$$\varphi : \Pi_1^2 \to \Pi_2^2 : P_1 \to P_2 := P_1^{\varphi} \text{ such that } \mathbf{G}_2 = \varphi^{-1}\mathbf{G}\varphi. \tag{3.3}$$

If the same φ above yields $\mathbf{N}_2 = \varphi^{-1}\mathbf{N}_1\varphi$, then $\mathbf{N}_1/\mathbf{G}_1$ and $\mathbf{N}_2/\mathbf{G}_2$ are also called equivariant. If $\mathbf{N}_2 > \varphi^{-1}\mathbf{N}_1\varphi$ then $\mathbf{N}_2/\mathbf{G}_2 > \mathbf{N}_1/\mathbf{G}_1$, i.e. $\mathbf{N}_2$ provides a richer symmetry group of $\Pi_2^2/\mathbf{G}_2$ than $\mathbf{N}_1$ provides that for $\Pi_1^2/\mathbf{G}_1$.

Isomorphic, i.e. equivariant normalizers $\mathbf{N}$'s of $\mathbf{G}$ form an equivalence class, and we are interested in determining the different classes and their subgroup relations. Here the relations of groups and maximal (proper) subgroups are satisfactory.

Any $\mathbf{G}$ (and $\mathbf{N}$) is defined (will be determined) by a fundamental (topological) polygon $\mathcal{F}_{\mathbf{G}}$ ($\mathcal{F}_{\mathbf{N}}$) with their side pairing isometries as generators, first in a combinatorial way, then metrically in a plane Π^2 by its signature. Hence the vertex classes with their stabilizers and the corresponding defining relations have been determined by a polygon symbol up to a combinatorial equivalence as indicated and illustrated above.

Although we may have many combinatorially different domains $\mathrm{F}_{\mathbf{G}}$ ($F_{\mathbf{N}}$) – our algorithm [9], [10], [11] enumerates all of them. Any $\mathrm{F}_{\mathbf{G}}$ by its barycentric subdivision and its **G**-images, at the neighbourhoods of non **G**-equivalent sides and vertices, by defining relations, gives us – in a finite algorithmic procedure – complete information on the systems of locally minimal closed geodesics as on the orientation preserving ones as on the orientation reversing ones and on their **G**-images as well. Any element n of a normalizer **N** maps these systems onto itself, now metrically if the domain $\mathrm{F}_{\mathbf{G}}$ is well deformed by a homeomorphism φ. Then we determine $\mathrm{F}_{\mathbf{N}}$ step by step.

At present we have not developed such an algorithm yet as GAP (see e.g. [1]) for automorphisms for certain finitely presented groups, but our method seems to be applicable to that problem and for certain general theory as mentioned in Remark 2.1–2.

Of course, any $\mathrm{F}_{\mathbf{G}}$ can be deformed in such a way that any possible normalizer **N** occurs, since any combinatorial $\mathrm{F}_{\mathbf{G}}$ can be cut and glue onto any other one by the usual topological procedure. But now we can concentrate on the cases where the **N**-images of $\mathrm{F}_{\mathbf{N}}$ tile $\mathrm{F}_{\mathbf{G}}$ by the representatives of $\mathbf{N}/\mathbf{G}$, and this is a finite procedure.

For $\mathbf{G} = \otimes^3$ we have 65 types of fundamental (topological) polygons as listed in Table 1 by computer. We examined each of them with the above respects of view. From the combinatorial structure of $\mathrm{F}_{\mathbf{G}}$ we selected a normalizer element and cut $\mathrm{F}_{\mathbf{G}}$ into a smaller domain with induced side pairing step by step, first by combinatorial line reflection, then by rotations especially by halfturn, glide reflection and translation, preserving the **G**-equivalence of sides. We always check the homomorphism criterion (see (2.7)) for any candidate **N** (see Fig. 8.a–b with 10/20 and 12/5, moreover Fig. 9.a–b for checking). Thus we obtain an $\mathrm{F}_{\mathbf{N}}$ and so **N** by its presentation, then $\mathbf{N}/\mathbf{G}$, moreover, the smallest $\mathrm{F}_{\mathbf{N}}$ for $\mathrm{F}_{\mathbf{G}}$, so the richest **N** and $\mathbf{N}/\mathbf{G}$ with tiling $\mathrm{F}_{\mathbf{G}}$ by the images of $\mathrm{F}_{\mathbf{N}}$ under representatives of $\mathbf{N}/\mathbf{G}$ as required.
In this way we obtained Table 2 from Table 1 by Table 3 and by a careful analysis.

Our most symmetric 12-gons for $\mathrm{F}_{\mathbf{G}}$ in Fig. 4.a–b illustrate the procedure. Fig. 4.a shows how to derive 12/2 **aabcddCeffEB** from the canonical side paired hexagon. By cutting along the edges of a tree graph, numbered by $1, \dots, 6$, we get 6 pieces. Then we glue them by the side pairing of the hexagon, considering also the vertex domains and the defining relation. Thus we get a 12-gon with the induced side pairing transformations and presentation

$$\mathbf{G} := (g_1, t_2, t_3, g_4, t_5, g_6 - \circ g_1 g_1 t_2, \blacksquare\, t_2 t_5^{-1} t_3^{-1}, \square\, g_4 g_4 t_3^{-1}, \bullet\, g_6 g_6 t_5^{-1}) = \otimes^3. \tag{3.4}$$

From this we read the invariant line system, e.g. the same line (along sides 1) for glide reflection g_1 and translation $t_2 = g_1 g_1$, and form the metric 12-gon with indicated angles at the vertices.

We promptly notice the maximal $\mathbf{D}_3$-symmetry of this combinatorial 12-gon and choose its metric data by the dihedral isometry group $\mathbf{D}_3$. But first we analyse the effect of introducing the line reflection m (in Fig. 4.a), only. Then we take an $\mathrm{F}_{\mathbf{N}_1}$ as any 7-gon, bounded by the reflection line segment on m. The generators of **G** in (3.4) induce a side pairing of the 7-gon:

a line reflection m_2 on side 2, since $mm_2 = t_2$, i.e. $m \sim m_2$ by $\mathbf{N}_1/\mathbf{G}$;

a point reflection M_1 in the midpoint M_1 of side 1, since $g_1 = M_1 m$, i.e. $m \sim M_1$ by $\mathbf{N}_1/\mathbf{G}$; the other side pairings with g_6 and $t_5 = g_6 g_6$ do not change, since $m g_6 m = g_4^{-1}$, $m t_5 m = t_3^{-1}$.

Thus, we get the presentation

$$\mathbf{N}_1 := (m, M_1, m_2, t_5, g_6 - m^2, M_1^2, m_2^2, mM_1m_2M_1, mt_5m_2t_5^{-1}, g_6g_6t_5^{-1}) =: \mathbf{2}{*}\otimes,\ |\mathbf{N}_1/\mathbf{G}| = 2 \quad (3.5)$$

with a polygon symbol (easy to understand, see Table 3).

$$F_{\mathbf{N}_1} \sim -\mathbf{a2A} - \mathbf{bccB},\ \text{and by } m \sim M_1 \sim m_2$$

$$\mathbf{N}_1/\mathbf{G} = \mathbf{D}_1 := (\overline{m} - \overline{m}^2) = \mathbf{C}_2 := (\overline{M}_1 - \overline{M}_1^2) = \mathbf{D}_1 = (\overline{m}_2 - \overline{m}_2^2). \quad (3.6)$$

This leads to exactly one tiling of the 3^- surface which can be derived from $F_\mathbf{G} = 10/12$ as well, if we glue the two 7-gons together at the midpoint M_1 by point reflection M_1 (see Fig. 1.d).

To introduce a 3-turn to our 12/2 we have 5 logically different possibilities for $F_{\mathbf{N}_2}$ with the same (equivariant) normalizer

$$\mathbf{N}_2 = (r, g_1, t_2 - r^3, g_1g_1t_2, (rt_2)^3) =: \mathbf{33}\otimes \quad (3.7)$$

where we have chosen $F_{\mathbf{N}_2}$ with two ■ vertices, representing a new 3-turn centre, $|\mathbf{N}_2/\mathbf{G}| = 3$.

To this $F_{\mathbf{N}_2}$ we could introduce the line reflections m' and m'' to get a new normalizer to $\mathbf{G}$ (Fig. 4.a)

$$\mathbf{N}_3 = (r, m', M, m'' - r^3, (m')^2, M^2, (m'')^2, m'rm''r^{-1},\ m'Mm''M) =: \mathbf{23}{*},\ |\mathbf{N}_3/\mathbf{G}| = 6 \quad (3.8)$$

with $F_{\mathbf{N}_3}$. But this $F_{\mathbf{N}_3}$ does not tile our 12-gon. Another one does that.

Now we introduce the line reflections m and $\widetilde{m}$ together (Fig. 4.a) to get the newer normalizer to $\mathbf{G}$ as follows

$$\mathbf{N}_4 := (m, M_1, m_2, \widetilde{m} - m^2, M_1^2, m_2^2, \widetilde{m}^2, mM_1m_2M_1, (m_2\widetilde{m})^3, (\widetilde{m}m)^3) = \mathbf{2}\,{*}\mathbf{33},\ (\mathbf{N}_4/\mathbf{G}) = 6. \quad (3.9)$$

The last possible extension of $\mathbf{N}_4$ to the maximal normalizer of $\mathbf{G}$ is the introduction of reflection m' to dissect $F_{\mathbf{N}_4}$ into two copies of domain $F_\mathbf{N}$. Hence we get $\mathbf{N}{=}{*}\mathbf{2223}$ with $|\mathbf{N}/\mathbf{G}| = 12$, as indicated formerly. $F_\mathbf{N}$ tiles our 12-gon by its representative $\mathbf{N}/\mathbf{G}$-images (see Fig. 1.a and Section 2).

Further extension of $\mathbf{N}$, to normalize $\mathbf{G}$, is not possible, because the only symmetry of $F_\mathbf{N}$ is the line reflection in OM_1 (Fig. 4.a), however, this does not preserve the invariant line system (locally minimal closed geodesics) of $H^2/\mathbf{G}$.

A similar discussion of the 12-gon in Fig. 4.b will no more be detailed. The first reflection m leads again to $\mathbf{N}_1 = \mathbf{2}{*}\otimes$ with combinatorially other domain.

The extension by 3-turn about centre O leads to $\mathbf{N}_2 = \mathbf{33}\otimes$ with various domains, again. In this case $\mathbf{N}_3 = \mathbf{23}{*}$, then $\mathbf{N}_4 = \mathbf{2}{*}\mathbf{33}$ and $\mathbf{N} = {*}\mathbf{2223}$ with appropriate tiling domains can also be constructed.

Table 1 contains the maximal normalizer for each $F_\mathbf{G}$, given by its polygon symbol, such that an $F_\mathbf{N}$ tiles $F_\mathbf{G}$ by its representative $\mathbf{N}/\mathbf{G}$-images. Tables 1 and 3 refer to each other in our classification of tilings for 3^- surface. Namely, from pieces of $F_\mathbf{N}$ we can glue an $F_\mathbf{G}$ with appropriate side pairings to obtain the fixed-point-free group $\mathbf{G} = \otimes^3$.

4. The Riemann-Hurwitz equation and the proof of non-existence

Although we have indicated the finiteness of symmetries of any compact surface, we cite an algorithmic procedure to prove this fact in a constructive way.

It is well-known [19] that the combinatorial measure of a surface of genus g^+ (orientable, $\alpha = 2$), or of genus g^- (non-orientable, $\alpha = 1$) is $4 - 2\alpha g$. Its fundamental group is denoted by $\mathrm{O}^g = \mathbf{G}$ or $\otimes^g = \mathbf{G}$, respectively.

The symmetry group $\mathbf{N}/\mathbf{G}$ is characterized by the normalizer $\mathbf{N}$ of $\mathbf{G}$ in $\mathrm{Isom}\,\Pi^2$. Π^2 is the hyperbolic plane H^2 if $2\alpha g > 2$, assumed now. $\mathbf{N}$ maps any $\mathbf{G}$-orbit onto itself.

Say, $\mathbf{N}$ has a signature (1.2) or (1.3) above, but with genus γ, orientability β. The combinatorial measure of $F_{\mathbf{N}}$ (or of $\mathbf{N}$) provides the *Riemann-Hurwitz formula*:

$$\frac{4-2\alpha g}{n} = 4 - 2\beta\gamma - 2\sum_{i=1}^{l}\Big(1-\frac{1}{h_i}\Big) - 2q - \sum_{j=1}^{q}\Big[\sum_{k=1}^{l_j}\Big(1-\frac{1}{h_{jk}}\Big)\Big], \tag{4.1}$$

i.e.

$$2\sum_{i=1}^{l}\frac{1}{h_i} + \sum_{j=1}^{q}\Big[\sum_{k=1}^{l_j}\frac{1}{h_{jk}}\Big] + \frac{2\alpha g - 4}{n} = -4 + 2\beta\gamma + 2q + 2l + l_1 + \cdots + l_q \tag{4.2}$$

holds as a necessary condition, where $\mathbf{N}/\mathbf{G} = n$ is the order of the group $\mathbf{N}/\mathbf{G}$. We assume for the (may be empty) rotation orders

$$2 \le h_1 \le \cdots \le h_l \in \Box \text{ (natural numbers)}, \tag{4.3}$$

for the dihedral corners (may be empty)

$$2 \le h_{jk} \in \Box;\ 1 \le j \le q,\ 1 \le k \le l_j. \tag{4.4}$$

The h_{jk}'s will be ordered first into non-decreasing sequence, then they will be reordered into (may be empty) cycles of the q boundary components by the given orientation ($\beta = 2$), or reordered into "circle" orders in non-orientable case ($\beta = 1$).

Furthermore, $h_i|n$ and $2h_{jk}|n$ hold as necessary divisibility conditions.

The equation (4.2) can be solved by a systematic algorithm for any fixed $2\alpha g$ by $\exp(g)$ complexity. See our case $\mathbf{G} = \otimes^3$ in Table 4.

Our non-existence proof is based on the 65 fundamental domains of $\mathbf{G} = \otimes^3$ in Table 1. The "algebraic" solutions in Table 4 provide the possible normalizers, for each candidate of them a fundamental polygon $F_{\mathbf{N}}$ with typical stabilizers (rotational and dihedral centres). These have to be "killed", as fixed points, by gluing n copies of $F_{\mathbf{N}}$ and by a new side pairing of the new fundamental domain for $\mathbf{G}$:

$$\mathsf{F}_{\mathbf{G}} = \bigcup_{i=1}^{n} \mathsf{F}_{\mathbf{N}}^{n_i}, \quad n_i \in \mathbf{N},\ \text{ representing } \mathbf{N}/\mathbf{G}. \tag{4.5}$$

But the side pairing has to be preserved by the symmetries of $\mathbf{N}$ according to the 65 possibilities in Table 1. In Table 4 we have just listed the 12 realizable solutions and the other non-realizable ones as well by careful analysis.

As a typical non-existence example, we choose solution $\langle 7\rangle *2*$, $n = 4$. In Fig. 10.a we consider a typical fundamental domain of $*2*$ [10] by polygon symbol

$$-2 - a - A = \mathsf{F}_{*\mathbf{2}*}. \tag{4.6}$$

By the maximal dihedral stabilizer **mm** of $*\mathbf{2}*$ we have to glue 4 copies of $\mathsf{F}_{*\mathbf{2}*}$ to have an $\mathsf{F}_{\mathbf{G}}$ with appropriate side pairing. Among the combinatorial octagons, however, we do not find any convenient side pairing whose **mm**-symmetries yield an $\mathsf{F}_{*\mathbf{2}*}$ domain. The candidates in Table 1 all exclude $\mathsf{F}_{*\mathbf{2}*}$.

Similarly in Fig. 10.b, we consider the solution $\langle 33\rangle$ $*\mathbf{255}$, $n = 20$. $\mathsf{F}_{*\mathbf{255}}$ is a reflection triangle with angles $\pi/2$, $\pi/5$, $\pi/5$. We have to find an appropriate side pairing for the double pentagon, i.e. octagon with 2 vertex classes, with angle sum 2π in each class, etc. We can not satisfy the necessary conditions without contradiction.

Of course, we might elaborate a general algorithm to obtain all the possible normalizers and their fundamental tilings for any g^--surface (and for any g^+-surface as well). The method of D-symbols seems to be effective for this reason (see [6]). Then we have to examine all possible $2g$-gons up to $6(g-1)$-gons as [10] indicated, but the procedure is of highly exponentional complexity by g [15].

6/1	aabbcc	2*33 / 3m, 6
2	aabcbC	$\otimes^3$ / 1, 1
3	aabcBC	2*$\otimes$ / m, 2
4	aabccb	2*222 / mm, 4
5	abacbc	*2224 / mm o m, 8
6	abacbC	2** / m, 2
7	abacBC	2** / m, 2
8	abcaBC	2*222 / mm, 4
8/1	aabbcddC	$\to$ 6/4
2	aabcbdCd	2*$\otimes$ / m, 2
3	aabcbddc	2*$\otimes$ / m, 2
4	aabcBdcD	222* / m, 2
5	aabcBdCD	2** / m, 2
6	aabcdbCd	2** / m, 2
7	aabcdBCD	2*$\otimes$ / m, 2
8	aabcdBdc	$\otimes^3$ /1, 1
9	aabcdcDB	$\to$ 6/6
10	aabcdCDB	$\to$ 6/5
11	aabcddcB	$\to$ 6/8
12	abacbdcD	$\otimes^3$ / 1, 1
13	abacbdCD	$\otimes^3$ / 1, 1
14	abacBdCd	2*$\otimes$ / m, 2
15	abacdbCD	2*$\otimes$ / m, 2
16	abacdbdc	*2223 / mm o 3, 12
17	abacdBcD	$\otimes^3$ / 1, 1
18	abAcdbDc	*22222 / mm, 4
19	abAcdBDc	*22222 / mm, 4
20	abcadBCD	2*$\otimes$ / m, 2
21	abcadcbD	2*$\otimes$ / m, 2
22	abcdaBcD	*2224 / 4m, 8
	and	*2223 / 2 o 3m, 12

10/1	aabcbdeeDc	$\to$ 10/16
2	aabccBdeeD	2*$\otimes$ / m, 2
3	aabcdbeCed	$\otimes^3$ / 1, 1
4	aabcdBeCDE	2*$\otimes$ / m, 2
5	aabcdBedcE	222* / m, 2
6	aabcdceDeB	$\to$ 8/16
7	aabcdCedEB	$\to$ 8/19
8	aabcdCeDEB	$\to$ 8/18
9	aabcdecDeB	$\to$ 8/18
10	aabcdeCDEB	$\to$ 8/16
11	aabcdeCedB	$\to$ 8/15
12	aabcdeeDcB	*2223 / m o 3m, 12
13	abacdbeCDE	$\otimes^3$ / 1, 1
14	abacdbedcE	$\otimes^3$ / 1, 1
15	abacdBceDe	2*$\otimes$ / m, 2
16	abacdBeCed	2*$\otimes$ / m, 2
17	abacdCbedE	222* / m, 2
18	abacdCbeDE	2** / m, 2
19	abacdeBcDe	2** / m, 2
20	abcadBeCDe	2*222 / m o 2, 4
21	abcadcebDE	$\otimes^3$ / 1, 1
22	abcadcedBE	2*$\otimes$ / m, 2
23	abcAdeBCEd	2*222 / mm, 4
24	abcAdecbEd	2*222 / mm, 4
12/1	aabcdceffEdB	2*$\otimes$ / m, 2
2	aabcddCeffEB	*2223 / 3m o m, 12
3	aabcdecfDfeB	$\to$ 12/11
4	aabcdeCfDEFB	$\to$ 10/23
5	aabcdeCfedFB	$\to$ 10/23
6	abacdeBcfDfe	2*$\otimes$ / m, 2
7	abacdeCbfDEF	2*$\otimes$ / m, 2
8	abacdeCbfedF	222* / m, 2
9	abcadeBdfCEf	*2223 / 3m o m, 12
10	abcadecfDbEF	2*$\otimes$ / m, 2
11	abcadecfeBdF	2*$\otimes$ / m, 2

Table 1. The list of fundamental domains for 3^- surface with their typical maximal tiling normalizers with factors and indices $|\mathbf{N}/\mathbf{G}|$

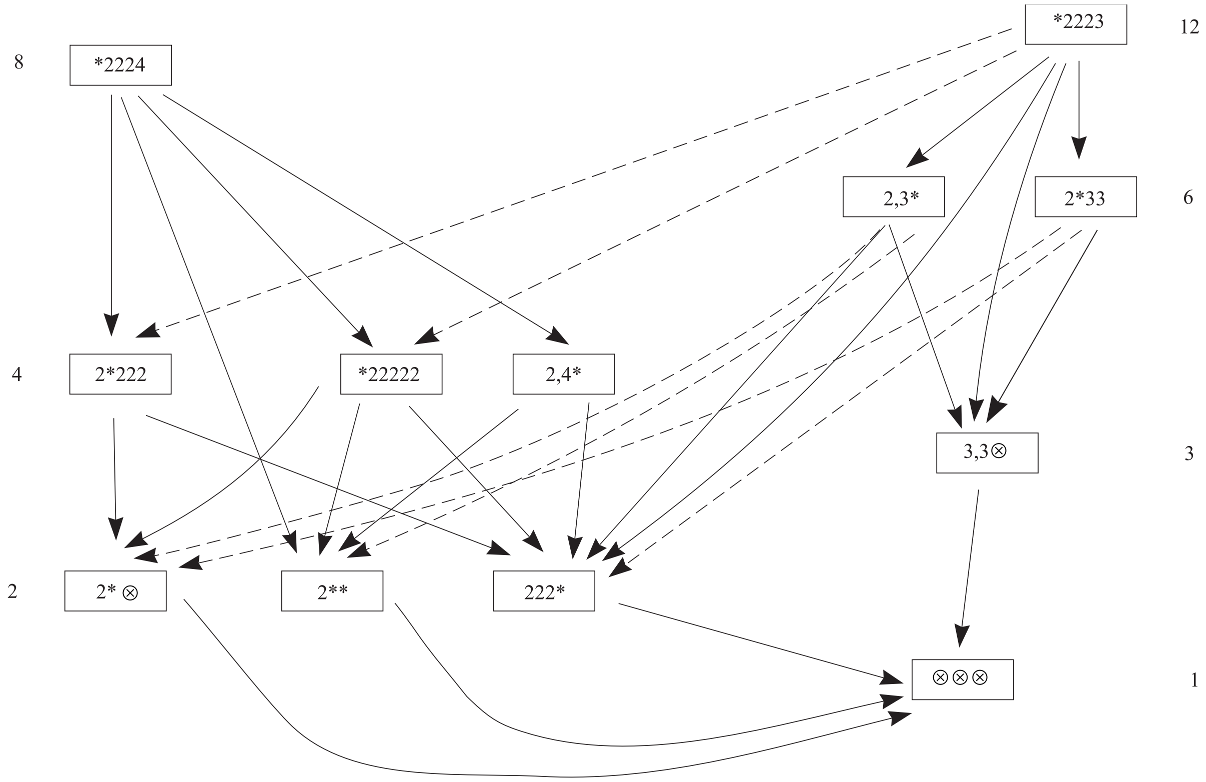

Table 2. Relations of (maximal) subgroups $\mathbf{N}/\mathbf{G}$ by normalizers $\mathbf{N}$: —— invariant ones - - - - noninvariant ones

222* (13 domains):	—a2Ab2Bc2C, —a2Ab2c2C2B, —a2b2B2c2CA, —a2b2c2C2B2A, —a2A—b2Bc2C, —a2A—b2c2C2B, —a2A—b2B—c2C, —a2Abc2Cd2DB, —ab2Bc2Cd2DA, —ab2Bc2d2D2CA, —a2bc2Cd2DB2A, —a2A—bc2cd2DB, —ab2Bcd2De2ECA
2 (4):**	—a2Ab—B, —a—A—b2B, —a2b—B2A, —ab—Bc2CA
2*⊗ (16):	— ab2Ba, —a2ba2b, —a2b2b2A, —a—ab2B, —a2b—a2b, —a—a—b2B, —abac2Cb, —abbAc2C, —abbc2CA, —abc2CbA, — ab2cb2cA, —a2bccBA, —a2A—bccB, —ab—ac2Cb, —ab2BcddCA, — abc2CdbdA
3,3⊗ (8):	a3a3b3B3, a3b3a3b3, aab3Bc3C, aab3c3C3B, a3Ab3cb3c, a3Abc3Cb, aabc3Cd3DB, a3ABc3CdBd
24* (5):	—a2Ab4B, —a4b2B4A, —a2b4B2A, —a2A—b4B, —ab2Bc4CA
***22222 (1):**	—2—2—2—2—2
2*222 (2):	—2—2—2a2A2, —2—2—2—a2A
2*33 (2):	—3—3a2A3, —3—3—a2A
23* (5):	—a2Ab3B, —a3b2B3A, —a2b3B2A, —a2A—b3B, —ab2Bc3CA
***2224 (1):**	—2—2—2—4
***2223 (1):**	—2—2—2—3

65+
58 tilings

Table 3. The list of polygon symbols $\mathcal{F}_\mathbf{N}$ by [11] for non-trivial normalizers $\mathbf{N}$ of $\mathbf{G} = \otimes^3$. In the symbols ... a ... a ... refers to side pairing by glide reflection ... b ... B ... refers to hyperbolic translation, — refers to line reflection; ... anb ... means rotation or dihedral centre of order n at joint of a and b, ... c2C ... refers to halfturn about the midpoint of a side, ... dnD ... refers to rotation of order n at joint of d and D.

$\boxed{1}$ $\langle 1 \rangle$ $\mathbf{N}=\mathbf{G}=\otimes^3$, $n=1$

I. $2\beta\gamma+2q=4$, $2l+l_1+\ldots+l_q\leq 2$

I.i $2l+l_1+\ldots+l_q=2$

I.i.1 $l=1$

$\langle 2 \rangle$ $2\ \otimes^2$, $n=2$; $\langle 3 \rangle$ $\square$ 2, $n=2$; $\boxed{2}$ $\langle 4 \rangle$ $\mathbf{2{*}\otimes}$, $n=2$; $\boxed{3}$ $\langle 5 \rangle$ $\mathbf{2{*}{*}}$, $n=2$

I.i.2 $l_1=2$ no solution

I.i.3 $l_1=1$ $l_2=1$ no solution

I.ii $2l+l_1+\ldots+l_q=1$

I.ii.1 $l_1=1$

$\langle 6 \rangle$ $*2\otimes$, n=4; $\langle 7 \rangle$ $*2*$, n=4,

II. $2\beta\gamma+2q=2$, $2l+l_1+\ldots+l_q\leq 6$

II.i $2l+l_1+\ldots+l_q=6$

II.i.1 $l=3$

$\langle 8 \rangle$ $222\otimes$, $n=2$; $\boxed{4}$ $\langle 9 \rangle$ $\mathbf{222*}$, $n=2$

II.ii $2l+l_1+\ldots+l_q=5$

II.ii.1 $l=2$, $l_1=1$

$\langle 10 \rangle$ $22{*}2$, $n=4$

II. ii.2 $l=1$, $l_1=3$

$\boxed{5}$ $\langle 11 \rangle$ $\mathbf{2{*}222}$, $n=4$;

II.ii.3 $l=0$, $l_1=5$

$\boxed{6}$ $\langle 12 \rangle$ $\mathbf{{*}22222}$, $n=4$;

II.iii $2l+l_1+\ldots+l_q=4$

II. iii.1 $l=2$

$\langle 13 \rangle$ $24\otimes$, $n=4$; $\boxed{7}$ $\langle 14 \rangle$ $\mathbf{24*}$, $n=4$; $\langle 15 \rangle$ $23\otimes$, $n=6$; $\boxed{8}$ $\langle 16 \rangle$ $\mathbf{23*}$, $n=6$;

$\boxed{9}$ $\langle 17 \rangle$ $\mathbf{33\otimes}$, $n=3$;

II.iii.2 $l=1, l_1=2$

$\langle 18 \rangle$ $2{*}23$, $n=12$; $\langle 19 \rangle$ $2{*}24$; $n=8$; $\boxed{10}$ $\langle 20 \rangle$ $\mathbf{2{*}33}$, $n=6$

II.iii.3 $l_1=4$

$\boxed{11}$ $\langle 21 \rangle$ $\mathbf{{*}2223}$, $n=12$; $\boxed{12}$ $\langle 22 \rangle$ $\mathbf{{*}2224}$, $n=8$; $\langle 23 \rangle$ $*2233$, $n=6$; $*2323$, $n=6$;

II.iv $2l+l_1+\ldots+l_q=3$

II.iv.1 $l=1$, $l_1=1$

$\langle 24 \rangle$ $3{*}4$, $n=24$; $\langle 25 \rangle$ $3{*}6$, $n=12$

II.iv.2 $l=0$, $l_1=3$

$\langle 26 \rangle$ $*237$, $n=84$; $\langle 27 \rangle$ $*238$, $n=48$; $\langle 28 \rangle$ $*2,3,9$, $n=36$;
$\langle 29 \rangle$ $*2,3,12$, $n=24$; $\langle 30 \rangle$ $*2,4,5$, $n=40$; $\langle 31 \rangle$ $*246$, $n=24$;
$\langle 32 \rangle$ $*248$, $n=16$; $\langle 33 \rangle$ $*2,5,5$, $n=20$; $\langle 34 \rangle$ $*266$, $n=12$; $\langle 35 \rangle$ $*334$; $n=24$; $\langle 36 \rangle$ $*336$, $n=12$; $\langle 37 \rangle$ $*444$, $n=8$

III. $2g+2q=0$ serves only orientable possibilities, no geometric realizations of normalizers for $\mathbf{G}=\otimes^3$

III.i $2l+l_1+\ldots+l_q=10$

III.i.1 $l=5$

$\langle 38 \rangle$ 22222, $n=2$

III.ii $2l+l_1+\ldots+l_q=8$

III.ii.1 $l=4$

$\langle 39 \rangle$ 2223, $n=6$; $\langle 40 \rangle$ 2224, $n=4$

III.iii $2l+l_1+\ldots+l_q=6$

III.iii.1 $l=3$

$\langle 41 \rangle$ 237, $n=42$; $\langle 42 \rangle$ 238, $n=24$; $\langle 43 \rangle$ 239, $n=18$; $\langle 44 \rangle$ $23,12$; $n=12$
$\langle 45 \rangle$ 245, $n=20$; $\langle 46 \rangle$ 246, $n=12$; $\langle 47 \rangle$ 248, $n=8$; $\langle 48 \rangle$ 255, $n=10$;
$\langle 49 \rangle$ 266, $n=6$; $\langle 50 \rangle$ 334, $n=12$; $\langle 51 \rangle$ 336, $n=6$; $\langle 52 \rangle$ 444, $n=4$

Table 4. The solution for Riemann-Hurwitz equation, $g^-=3$, $\alpha=1$, $\mathbf{G}=\otimes^3$. $\square$ indicates proper normalizer $\mathbf{N}$, $\langle\ \rangle$ for algebraic solution

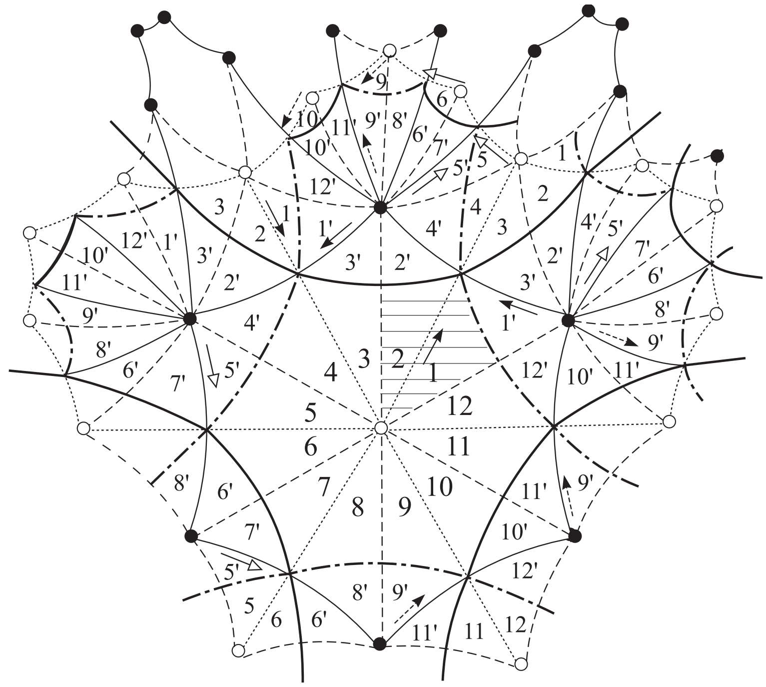

a)

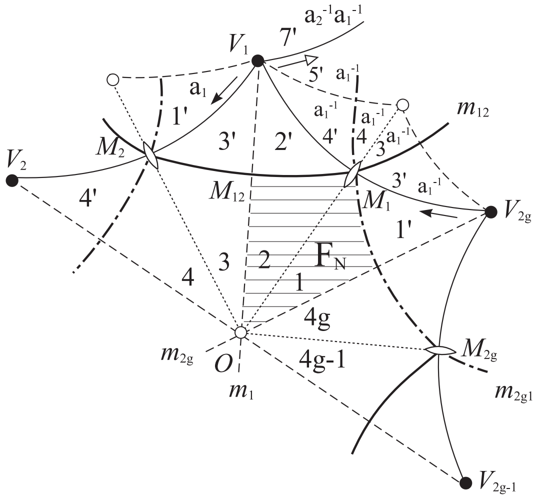

b)

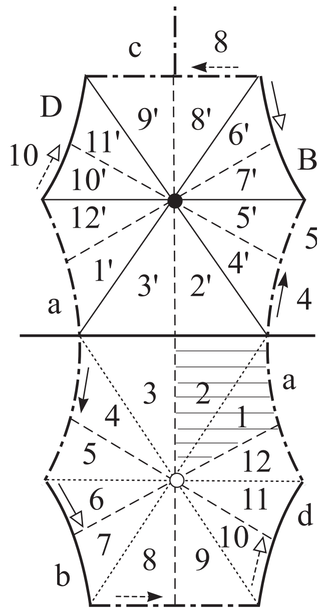

c) 8/22: abcdaBcD

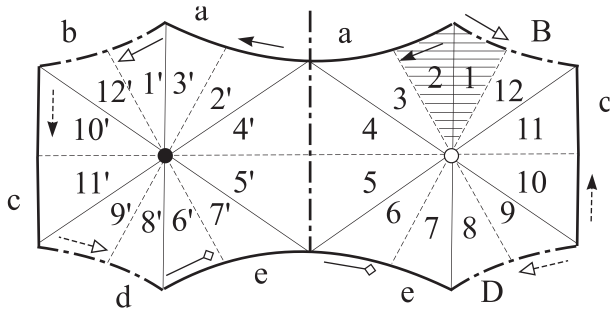

d) 10/12: aabcdeeDcB

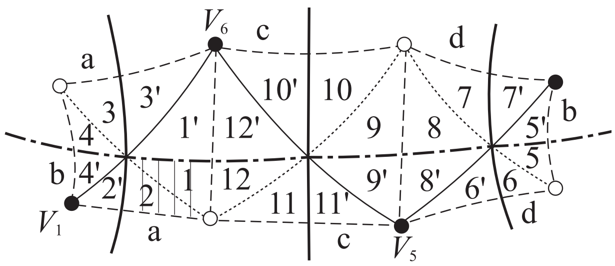

e) 8/16: abacdbdc

Figure 1. a) The 6/1 tiling of polygon symbol **aabbcc**, its barycentric subdivision; b) maximal normalizer for g^- surface, $g = 3$, its fundamental domain $\mathcal{F}_\mathbf{N} = (1, 2)$; c)–e) some domains for 3^- surface with tilings by $\mathcal{F}_\mathbf{N}$

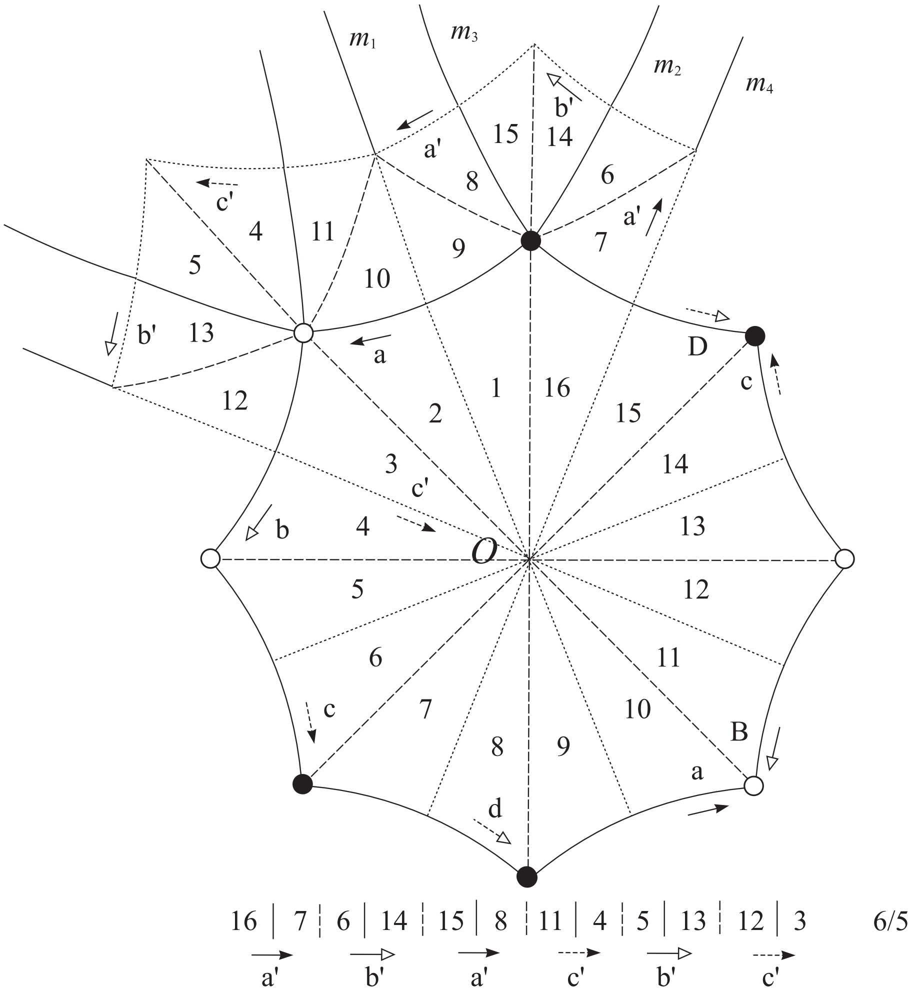

a) 8/22: abcdaBcD

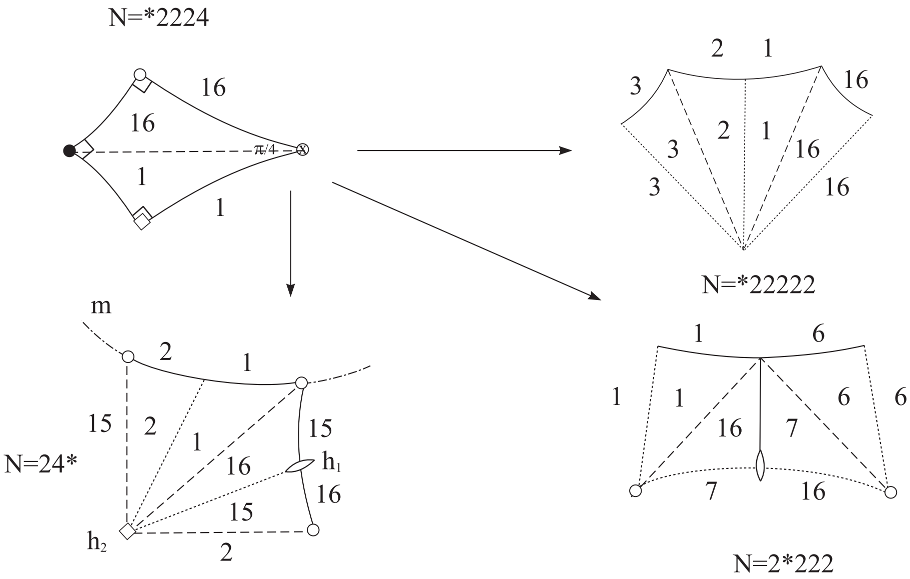

b)

Figure 2. a) Derivation of a hexagon from an octagon and vice versa; b) the subgroup relation of normalizers $*2224 \triangleright 24*$, $*2224 \triangleright 2*222$ and $*2224 \triangleright *22222$, respectively

	$\|\mathbf{N}/\mathbf{G}\|$	F_N	Conway-Macbeath Signature of a typical **N**
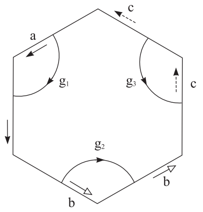 aabbcc $g_1g_1g_2g_2g_3g_3=1$	12	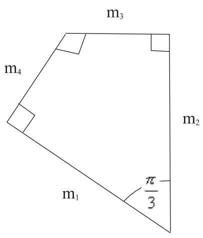	*2223
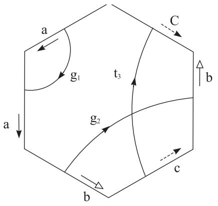 aabcbC $g_1g_1g_2t_3g_2^{-1}t_3=1$	2	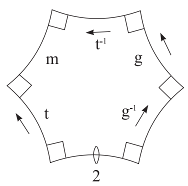	2*⊗
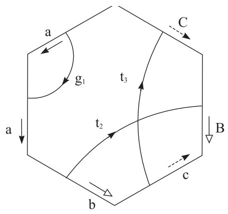 aabcBC $g_1g_1t_2t_3^{-1}t_2^{-1}t_3=1$	4	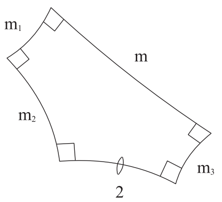	2*222

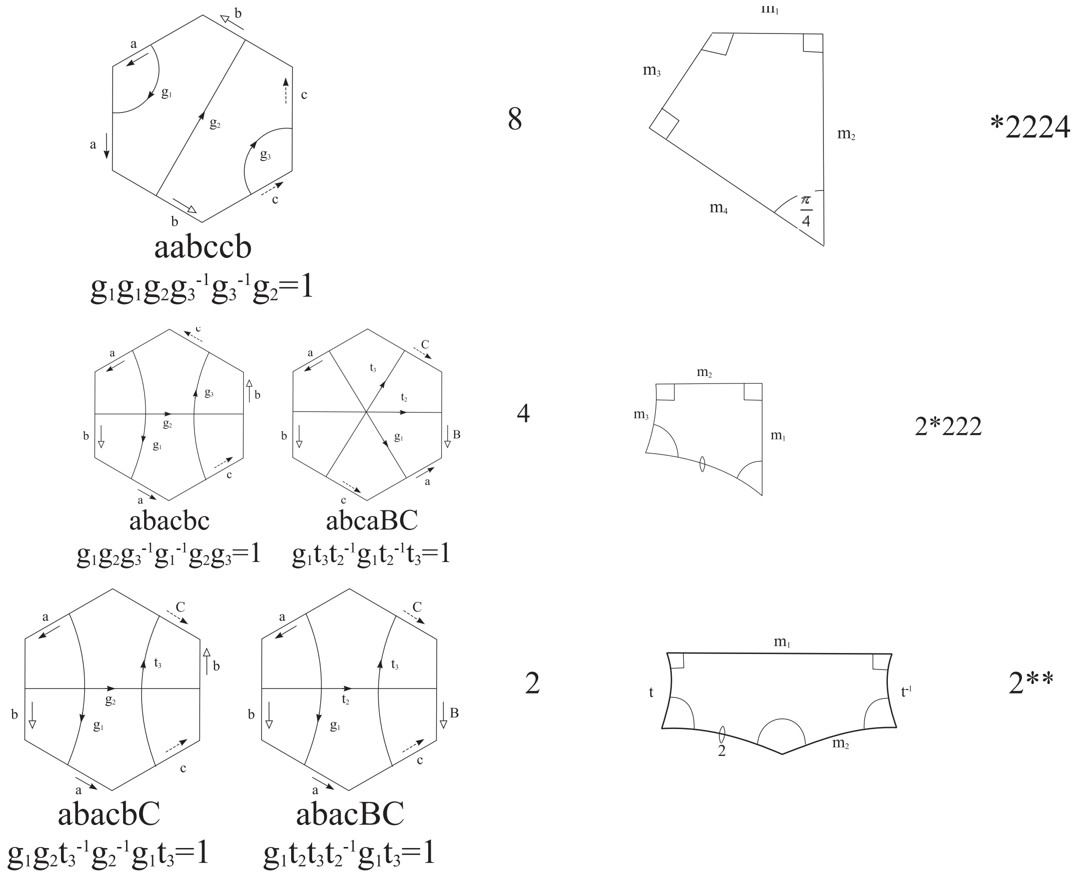

Figure 3. Hexagonal domains with generating closed geodesics and some typical normalizers for the 3^- surface from [16]

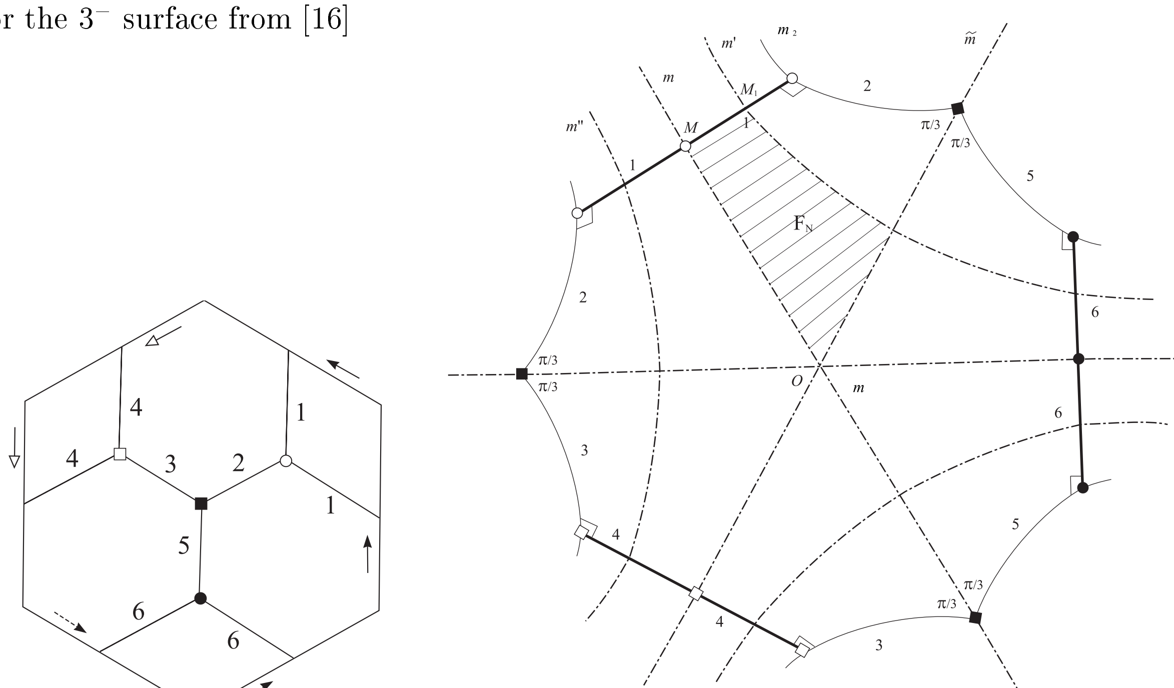

a)

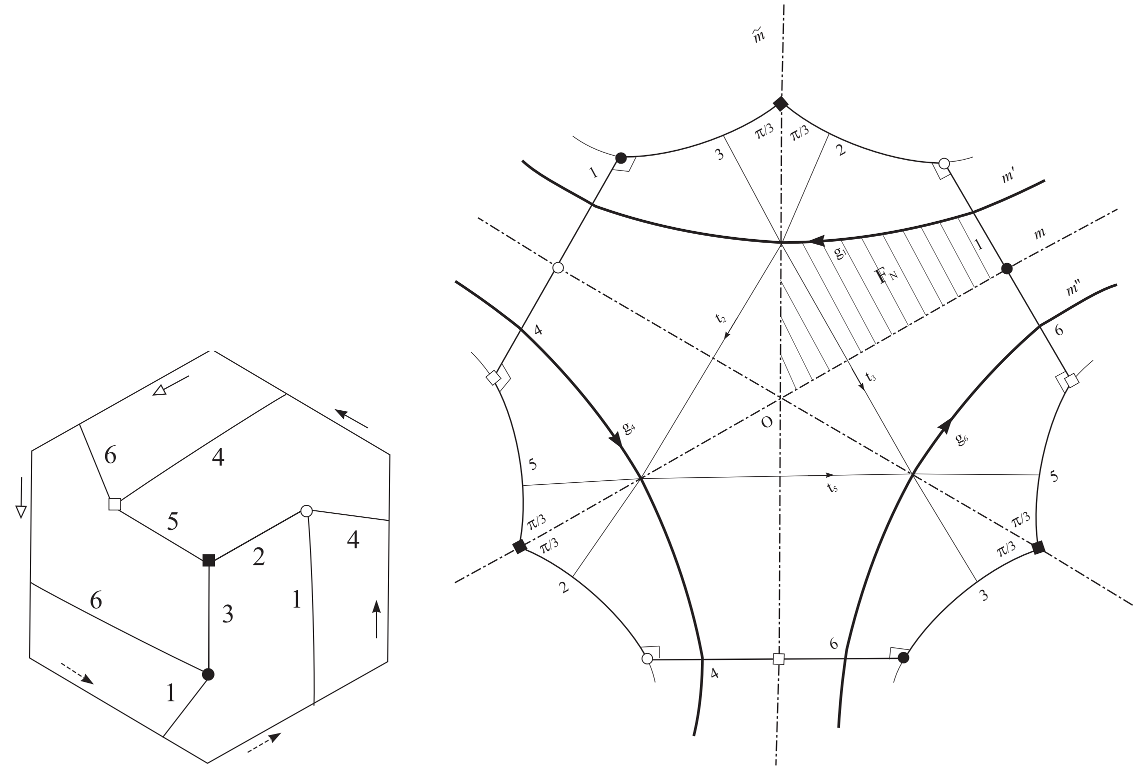

b)

Figure 4. a) Two 12-gonal fundamental domains for $\mathbf{G} = \otimes^3$ with maximal normalizer $\mathbf{N} = *\mathbf{2223}$ leading to equivariant tilings. a) 12/2: **aabcddCeffEB**; b) 12/9: **abcadeBdfCEf**

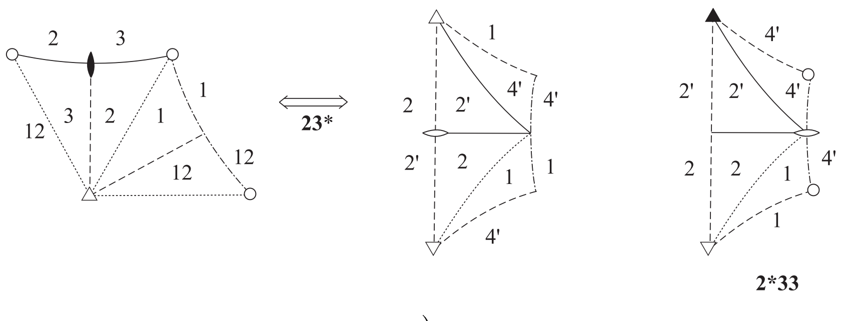

a)

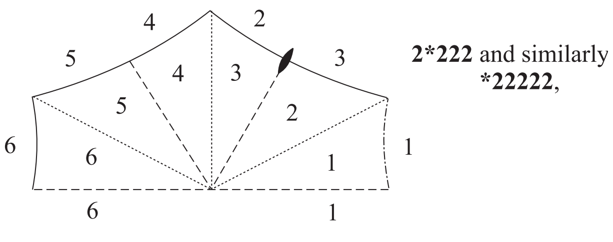

b)

Figure 5. Maximal subgroups of $*\mathbf{2223}$ by Fig. 1.a; a) of index 2; b) of index 3 (non-invariant)

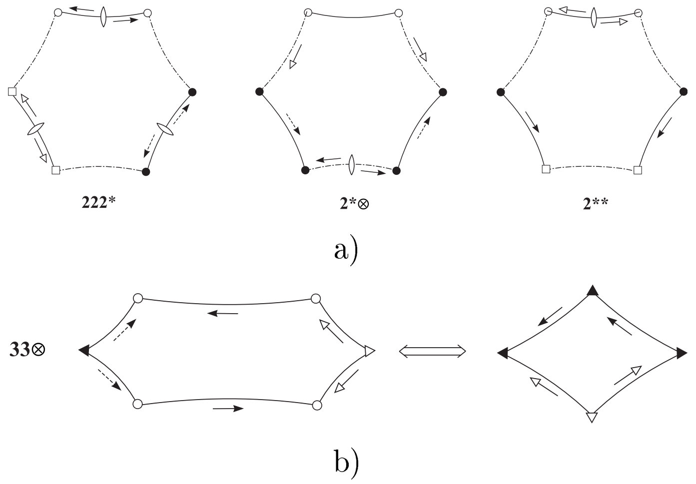

Figure 6. Maximal subgroups of $\mathbf{23}*$; a) of index 3; b) of index 2.

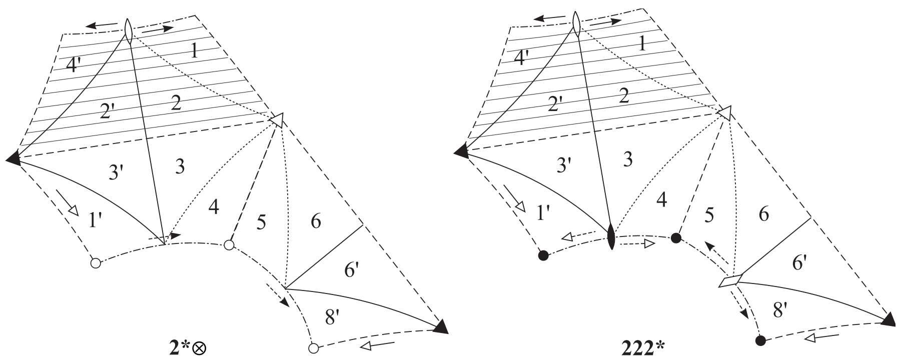

Figure 7. Maximal non-invariant subgroups of $\mathbf{2{*}33}$ of index 3

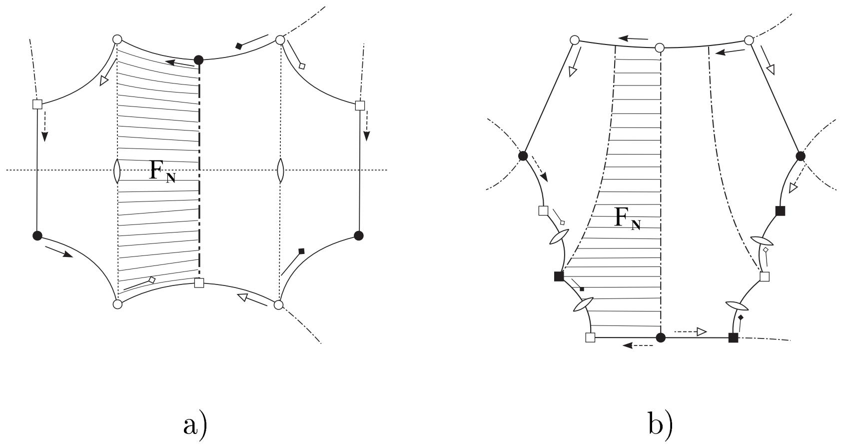

Figure 8. Extreme symmetries a) by glide reflection 10/20: **abcadBeCDe**, $\mathbf{N} = \mathbf{2{*}222}$; b) by translation 12/5: **aabcdeCfedFB**, $\mathbf{N} = \mathbf{2{*}222}$

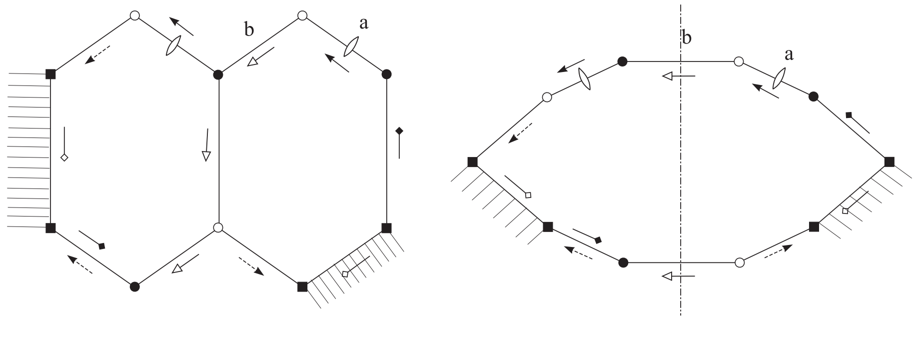

a) b)

Figure 9. Extension of $\mathcal{F}_{\mathbf{G}}$ 10/19: **abacdeBcDe** to $\mathcal{F}_{\mathbf{N}}$; a) by glide reflection to $\mathbf{N} = \mathbf{2}{*}\otimes$, b) by reflection to $\mathbf{N} = \mathbf{2}{*}{*}$

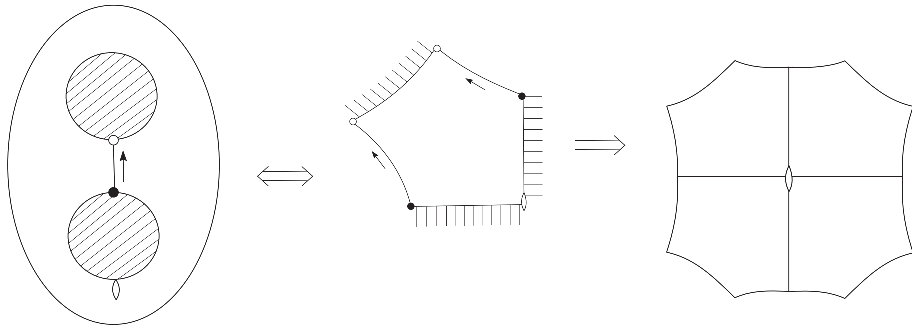

a)

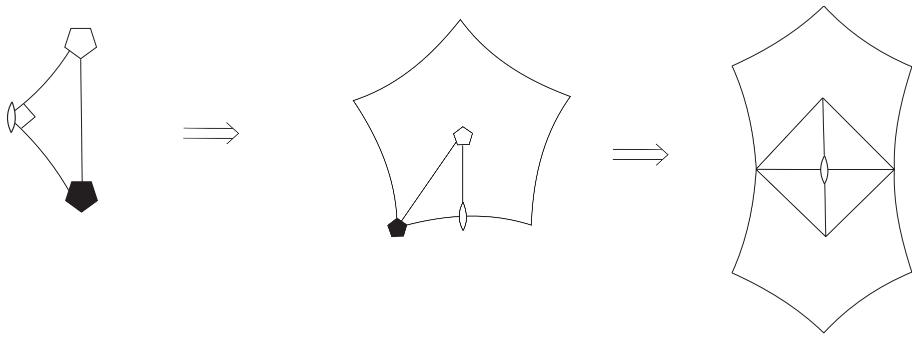

b)

Figure 10. a) Non-existence for $*\mathbf{2}*$, b) for $*\mathbf{255}$

References

[1] Breuer, T.: *Characters and automorphism groups of compact Riemann surfaces*. London Math. Soc. Lect. Note Ser. **280**, Cambridge Univ. Press 2000. Zbl 0952.30001

[2] Bilinski, S.: *Homogene mreže zatvorenih orientabilnih ploha*. Rad, Jugosl. Akad. Znan. Umjet. **277** (1951), 129–164.
Homogene Netze geschlossener orientierbarer Flächen. Bull. Int. Acad. Yugosl. **6** (1952), 59–75.

[3] Conder, M. D. E.: *The genus of compact Riemann surfaces with maximal automorphism group*. J. Algebra **108** (1987), 204–247. Zbl 0614.20035

[4] Casson, A. J.; Bleiler, S. A.: *Automorphisms of surfaces after Nielsen and Thurston*. London Mathematical Society Student Texts **9**, Cambridge Univ. Press 1988. Zbl 0649.57008

[5] Dress, A. W. M.; Franz, R.: *Zu einer Frage von Herrn S. Bilinski, Pflasterungen von Brezelflächen betreffend*. Rad, Jugosl. Akad. Znan. Umjet **428** (1987), 83–101. Zbl 0649.52008

[6] Franz, R.; Huson, D. H.: *The classification of quasi regular polyhedra of genus 2*. J. Discrete Comput. Geom. **7** (1992), 347–357. Zbl 0752.52006

[7] Huson, D.: *The generation and classification of tile-k-transitiv tilings of the euclidean plane, the sphere and the hyperbolic plane*. Geom. Dedicata **47** (1993), 269–296. Zbl 0787.52011

[8] Karcher, H.; Weber, M.: *On Klein's Riemann surface*. Manuscript 1996.
The geometry of Klein's Riemann surface. The eightfold way. Math. Sci. Res. Inst. Publ. **35**, 9–49, Cambridge Univ. Press, Cambridge 1999. Zbl 0964.14029

[9] Lučić, Z.; Molnár, E.: *Combinatorial classification of fundamental domains of finite area for planar discontinuous isometry groups*. Arch. Math. **54** (1990), 511–520. Zbl 0708.57016

[10] Lučić, Z.; Molnár, E.: *Fundamental domains for planar discontinuous groups and uniform tilings*. Geom. Dedicata **40** (1991), 125–143. Zbl 0745.52012

[11] Lučić, Z.; Molnár, E.; Vasiljević, N.: *Combinatorial structure of fundamental polygons of finite area for plane discontinuous groups*. Manuscript 1998.

[12] Molnár, E.: *Polyhedron complexes with simply transitive group actions and their metric realizations*. Acta Math. Hung. **59** (1992), 175–216. Zbl 0810.57027

[13] Ratcliffe, J. G.: *On the isometry groups of hyperbolic manifolds*. Contemp. Math. **169** (1994), 491–495. Zbl 0809.30039

[14] Senechal, M.: *Tiling the torus and other space forms*. Discrete Comput. Geom. **3**(1) 1988, 55–72. Zbl 0627.05046

[15] Stettner, E.: *Die computergestützte Klassifizierung der Flächeneinwickelungen in einem Vieleck vorgegebener Seitenanzahl*. Annales Univ. Sci. Budapest **41** (1998), 103–115. Zbl 0940.52008

[16] Stettner, E.: *Symmetriegruppen und fundamentale Pflasterungen der Fläche vom Geschlecht -3. I. Maximale Gruppen mit Sechseckbereichen.* Studia Sci. Math. Hung. **40** (2003), 41–57. Zbl pre02099019

[17] Schmutz Schaller, P.: *Geometry of Riemann surfaces based on closed geodesics.* Bull. Am. Math. Soc. (New Ser.) **35**(3), 193–214. Zbl 1012.30029

[18] Zamorzaeva, E.: *On isohedral tilings of hyperbolic manifolds.* An. Stiint. Univ. Al. I. Cuza Iasi. Mat. (Ser. Nouva) **43**(1) (1997), 81–88 (1996). Zbl 0974.52018

[19] Zieschang, H.; Vogt, E.; Coldewey, H.: *Surfaces and Planar Discontinuous Groups.* Springer, Berlin Heidelberg New York 1980. Zbl 0438.57001

Received June 5, 2003